# Transient Viscosity and Molecular Order of a Thermotropic Polyester LCP in Uniaxial Elongational Flow

**William A. Kernick III and Norman J. Wagner***

*Center for Molecular and Engineering Thermodynamics, Department of Chemical Engineering University of Delaware, Newark, Delaware 19716*

*Received May 15, 1998; Revised Manuscript Received December 28, 1998*

ABSTRACT: The transient elongational viscosity and molecular orientation are measured for a TLCP under simple uniaxial elongational flow. Substantial strain hardening is observed for Hencky strains greater than one, with both the molecular order and transient elongational viscosity becoming independent of strain rate. The transient elongational viscosity is observed to follow a master curve in this regime, scaling as strain squared. X-ray scattering measurements of the orientational order parameter show the strong orienting ability of elongational flows. The quantitative results are compared to those of simple shear flow, as well as to molecular theories, showing important deviations from the behavior expected for model, rigid rod nematics.

## Introduction

Thermotropic liquid-crystalline polymers (LCPs) are candidates for use as high temperature, high strength materials.[1] They have also found extensive use in high precision parts, such as electrical connectors, due to their ease in mold filling, low coefficient of thermal expansion, and low flash.[2] Their high cost and difficulty in processing have also driven research into blending with other engineering thermoplastics.[3] The strength of main-chain LCP-based materials is governed by the molecular order and its orientation, such that control of this anisotropy is often key to the successful application of LCPs. Polymer processing operations often involve converging flow, fiber spinning, or blow molding, all flows with substantial elongational character. Thus, understanding the coupling between the transient LCP rheology and the evolving anisotropy under elongational conditions is of practical importance, as well as of basic scientific interest.

The liquid crystalline molecular structure and mesoscopic texture, the latter often envisioned as a "domain" structure, inherent in LCPs are responsible for their unique rheology. This rheology is reviewed for model, main-chain LCPs in the recent paper by Mewis and Moldenaers[4] and the chapter by Marrucci and Greco.[5] The LCP character is manifest in scaling laws for the transient shear response, specifically, that the reduced stress scales with strain in the low-shear, pseudo-Newtonian plateau ("region II").[4,6,7] At higher shear rates comparable to the inverse rotary diffusion time of the molecules, shear thinning and a loss of strain scaling for the transient shear viscosity is observed.[8] Similar experimental evidence for universal LCP behavior in elongational flows has not been established.[9,10]

The rheology of LCPs can be largely interpreted in terms of the net molecular orientation under flow.[6,7] This is quantified as a scalar order parameter ($S$), giving the net uniaxial orientation of the molecules relative to the average direction of orientation ("director"). Note that, in general, this parameter is a convolution of the actual molecular order with the mesoscale texture in the bulk material.[21] An order parameter of zero denotes a net, isotropic system, while an order parameter of unity is perfectly aligned. The order parameter can be measured under flow and for samples quenched during flow for both melts and solutions by several measurement techniques. Of relevance here is X-ray scattering, which has been employed in studies of shear[12−14] and elongational flows.[13,15,16] We note that studies using small angle neutron scattering,[12,17] birefringence,[12,18] and FTIR[16] have also been reported. These studies generally report an effective, overall order parameter that increases with increasing shear rate or draw ratio, indicating that the LCP becomes more aligned in the flow direction with increasing flow strength. A more complex behavior is observed at lower shear rates, where tumbling and defect dynamics become important.[12,17] Generally, drawing samples is observed to produce much higher orientations than shearing at comparable rates, as has been demonstrated by Picken et al.[13] Elongational viscosities have been measured for polymer melts using a variety of techniques, including fiber spinning, converging flow, and rotary clamp methods.[19,20] Recent advances in the accurate measurement of the transient elongational viscosity during uniaxial elongation[21] using a rotary clamp-style device have made it possible to study the evolving elongation behavior of TLCPs under controlled temperature and flow conditions over a wide range of strains and strain rates. This instrument was employed by Gramspacher and Meissner[22] to study polymer blends and by Levitt et al.[23] to study polymer interfaces.

There have been substantial elongational rheology investigations on polyolefin melts: polyethylene (LDPE and HDPE)[24−26] and polypropylene,[27] where in these systems the deviation from linear viscoelasticity (strain-hardening) increased with increasing branching. For lyotropic liquid crystalline polymers, there has been work on solutions using spinning[9] and filament drawing[28] methods, where no strain-hardening was observed. Wagner and co-workers recently[29] measured the elongational viscosity using a Rheotens fiber-spinning measurement on a commercial TLCP (Vectra B950) and noted a behavior similar to polyethylene. However, the flow was neither viscometric nor was the experiment

* Corresponding author. Email: wagner@che.udel.edu.

10.1021/ma980780k CCC: $18.00 
Published on Web 02/04/1999

isothermal. Wilson and Baird[10] measured transient elongational viscosity on two TLCPs (Vectra A900 and hydroxypropylcellulose) in both nematic and isotropic states using a rotating clamp device and observed strain-hardening. However, they attributed the strong strain-hardening to residual crystallinity rather than an innate LCP property. These disparate results may partially be a consequence of experimental geometry and interpretation or actual differences in materials; resolving these differences will require quantifying the molecular structure of the polymers during elongation and comparison to established molecular models for idealized rigid-rod nematics.

In this work we report the first measurements of both the transient, isothermal elongational viscosity of a TLCP and the molecular order parameter. Fiber X-ray scattering techniques are employed to measure the degree of molecular alignment induced by the elongational flow. These results are compared to previous studies of the same polymer under shear flow to evaluate the relative importance of elongation on the LCP microstructure and rheology. Further, the results are compared to solutions of the Doi model[6] to ascertain the ability of molecular theories to interrelate steady shear and elongational flow in TLCPs. The results provide interpretation for the empirical evidence concerning the behavior of LCPs in various polymer processing operations.

## Experiment

The thermotropic copolyester LCP used here, HX-8000−210 (DuPont),[30] is the same polymer studied previously by van Eijndhoven-Rivera et al.[14] The LCP has a nominal melting temperature of 210 °C as determined by DSC and rheological measurement. As per the previous work, the LCP was dried then melt-filtered at 290 °C using a twin-screw extruder with a vacuum port and a screen pack prior to subsequent preparations. The polymer pellets thus formed were dried for a minimum of 12 h at 110 ° C under vacuum prior to any molding. For the elongational rheometry, the pellets were pressed into a square mold at 240 °C and then milled to the dimensions required for the elongational rheometer: approximately a 7 mm × 1.5 mm rectangular cross-section by 56 mm length sample. All elongational experiments were conducted with samples prepared from the same pressing.

For the rotational rheometry, 2.54 cm circular wafers were stamped from the same pressed sheet as used for the elongational samples. Additional wafers were made by following a similar pressing protocol, but were cut to size using a circular die. Prior to both elongational and shear rheometry measurements the samples were dried for at least 12 h at 110 ° C under vacuum.

The elongational rheometry was performed at The Swiss Federal Institute of Technology Rheocenter (ETH, Zürich) using a constant rate elongational rheometer, previously described by Meissner and Hostettler[21] with modification as described by Levitt et al.[23] The rheometer is commercially available from Rheometrics (Piscataway, NJ) under the name RME. A solid sample was loaded into the heated sample chamber (240 °C) and clamped between the double belt clamp system. The sample is heated and supported by a nitrogen gas flow. After 5 min, the molten polymer sample was subjected to a constant elongation rate to a maximum Hencky strain of $\epsilon = 5$. Glass beads were dispersed onto the molten sample prior to elongation, and the position of the beads was followed with a camera system and imaging software. Particle tracking the bead positions verified both the rate and homogeneity of the elongation. All of the measurements reported here were homogeneous in elongational rate across the length and width of the sample. The elongation strain rate is held constant for each experiment, such that the total (Hencky) strain is given by eq 1, where $l(t)$ indicates the sample length at time $t$, and

$$\epsilon(t) = \dot{\epsilon} t = \ln\left(\frac{l(t)}{l_0}\right) \tag{1}$$

$l_0$ the same at time zero. Since the melt is assumed to be incompressible, the change of cross-sectional area, $A(t)$, is given by eq 2,

$$A(t) = A_0 \exp(-\dot{\epsilon} t) \tag{2}$$

where $A_0$ is the cross-sectional area at time zero. The cross-section of the sample at the test temperature was determined by correcting the room-temperature measurements (±0.01 $mm$), by a thermal expansion coefficient of $2.5 \times 10^{-4}$ length$^2$/$C$.[31] The tensile stress, $\sigma_E(t)$, is calculated by dividing the measured force, by the calculated cross-sectional area, yielding the instantaneous elongational viscosity:

$$\eta_E(t) = \frac{\sigma_E(t)}{\dot{\epsilon}(t)} \tag{3}$$

The rotational rheometry was performed on a Rheometrics (Piscataway, NJ) RMS-800 controlled strain rheometer with a 25 mm 0.1 rad angle cone and plate tooling. A heated nitrogen gas stream maintained an inert atmosphere at the test temperature (240 °C). After loading, samples were subjected to a preshear protocol of steady shear at 0.5 for 1000 s followed by 1000 s of relaxation. The preshear protocol ensured a reproducible starting state for the rotational rheometry, and removed any sample structure induced by the loading. The comparisons between shear and elongational results are done at equal second invariants of the strain rate tensor,[32,33] which translates to $\dot{\gamma}$ for simple shear, and $\sqrt{3}\dot{\epsilon}$ for the uniaxial elongation.

Some RME test samples were quenched immediately upon flow cessation by clamping at both ends, cutting, and quenching into ice water. Two-dimensional X-ray scattering images were obtained on the same X-ray diffractometer described by van Eijndhoven-Rivera et al.[14] The instrument consists of a Phillips tube generator with a graphite monochromator (Cu Kα radiation with 1.54 Å wavelength) and an image plate detector. The resulting image was digitized using a Molecular Dynamics scanner with a 100 $\mu$m resolution. Sample to detector distance was 5 cm, and the run collection time for each image was 60 min.

The effective order parameter of LCP quenches was determined using the following methodology. First, the constant background due to instrument and incoherent scattering was empirically determined using a $Iq^4$ vs $q^4$ Porod-style plot of the circularly averaged pattern at high $q$, and subtracted from the measured patterns. The anisotropy in the resulting 2D patterns was quantified by performing azimuthal scans at a fixed scattering angle, taken at the $|\mathbf{q}|$ corresponding to the maximum intensity Following the approach of Picken et al.,[13] the azimuthal scans were fit to eq 4,

$$I_{meas}(\mathbf{q}) = I(q,\Psi) + B = I_{max}(q) \exp(\alpha(P_2(\cos\Psi) - 1)) + B \tag{4}$$

where $I_{max}$ is the maximum intensity, α is a fitting parameter, $P_2(\cos\Psi) = {}^1/_2(3\cos^2(\Psi) - 1)$ is the second Legendre polynomial, $B$ is the experimentally determined background value, and Ψ is the azimuthal angle defined as zero at the maximum scattered intensity. Due to the Fourier transform relationship between real-space structure and the scattering, $\Psi = 90°$ corresponds to the elongational direction. The fit parameter α is related to the effective order parameter through eq 5, using eq 4 for the intensity.

$$S_{eff} = \frac{\int_0^{2\pi} I(\Psi) P_2(\cos\Psi) \sin\Psi \, d\Psi}{\int_0^{2\pi} I(\Psi) \sin\Psi \, d\Psi} \tag{5}$$

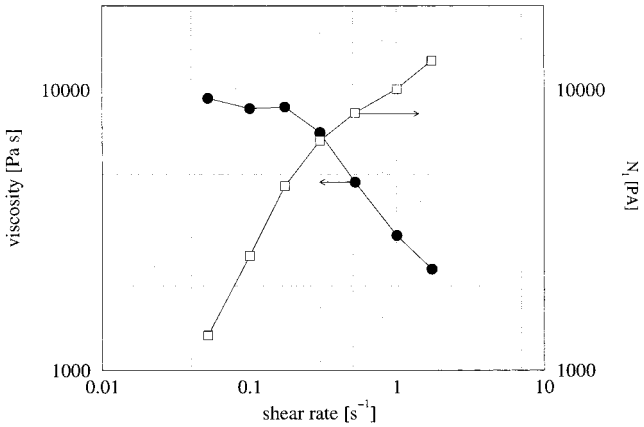


**Figure 1.** Steady shear viscosity (●) and first normal stress difference (□) as a function of rate for LCP210 at a test temperature of 240 °C.

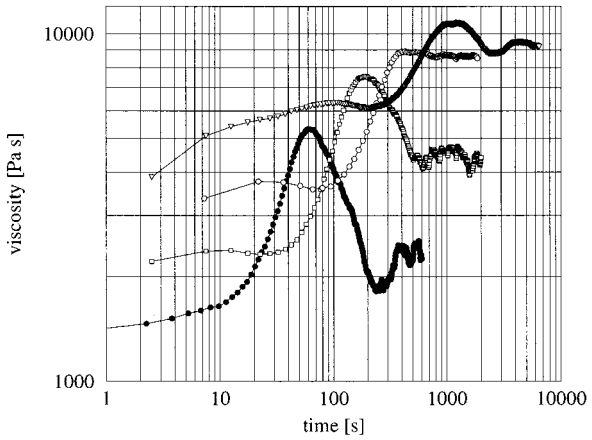


**Figure 2.** Transient shear viscosity for various shear rates as a function of time at 240 °C: $\dot{\gamma} = 1.73\ s^{-1}$ (●), $\dot{\gamma} = 0.52\ s^{-1}$ (□), $\dot{\gamma} = 0.173\ s^{-1}$ (○), $\dot{\gamma} = 0.052\ s^{-1}$ (▽).

## Results and Discussion

**Rheology.** The steady shear viscosity and first normal stress difference as a function of shear rate are shown in Figure 1, exhibiting behavior typical of main-chain TLCPs.[34−36] The viscosity curve is more complex then that of model, lyotropic LCPs, lacking a clear pseudo-Newtonian region at intermediate shear rates.[37] This is followed by a shear thinning region (power law $n = 0.35$) at higher shear rates. The first normal stress difference scales linearly with shear rate at low rates, which is again typical of LCPs.[6] When the shear viscosity shear thins, the first normal stress difference deviates sublinearly, but does not show signs of decreasing, as is observed in model LCPs.[38,39] The transient shear viscosity is shown in Figure 2 as a function of time and Figure 3 as a function of strain. The observed stress overshoot is qualitatively similar to that observed in model lyotropic LCPs.[11,40,41] However, as is typical of thermotropic LCPs, the scalings with strain are not as evident as for the model lyotropic LCPs.[42]

The transient elongational viscosity for various applied elongational rates is shown in Figure 4. The material initially exhibits weak strain hardening, followed by extreme strain hardening at longer times.

Also included in Figure 4 is three times the measured transient shear viscosity for the lowest shear rate tested in the rotational rheometer (0.052, equivalent to 0.03). The elongational viscosity clearly exceeds a Trouton ratio of 3 for the entire transient, in agreement with

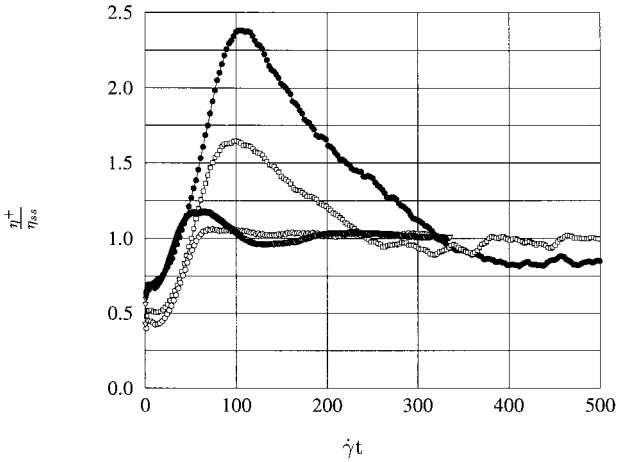


**Figure 3.** Scaled transient shear viscosity for various shear rates as a function of strain ($\dot{\gamma}t$) at 240 °C: $\dot{\gamma} = 1.73\ s^{-1}$ (●), $\dot{\gamma} = 0.52\ s^{-1}$ (□), $\dot{\gamma} = 0.173\ s^{-1}$ (○), $\dot{\gamma} = 0.052\ s^{-1}$ (▽).

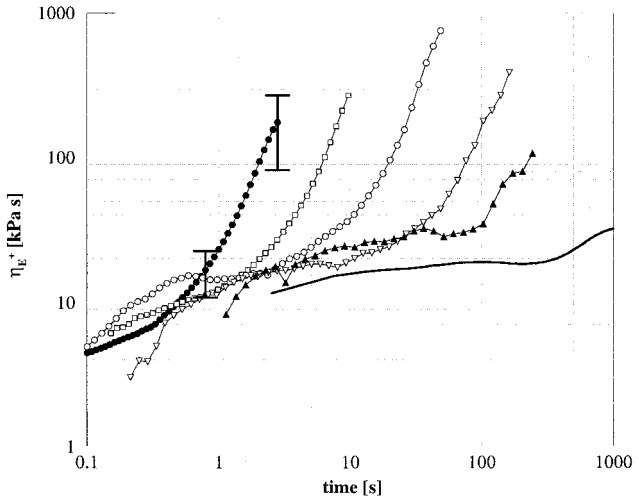


**Figure 4.** Transient elongational viscosity for various elongational rates at 240 °C: $\dot{\epsilon} = 1.0\ s^{-1}$ (●), $\dot{\epsilon} = 0.3\ s^{-1}$ (□), $\dot{\epsilon} = 0.1\ s^{-1}$ (○), $\dot{\epsilon} = 0.03\ s^{-1}$ (▽), $\dot{\epsilon} = 0.01\ s^{-1}$ (▲). The solid line is $3\eta^+$ as obtained from transient shear experiment at $\dot{\gamma} = 0.052\ s^{-1}$, which corresponds to $\dot{\epsilon} = 0.03$. Characteristic error bars are shown.

previous studies of LCP solutions.[9] Given the importance of sample rheological history, this result is not suprising due to the differences between sample histories between shear and elongational experiments. Note that the elongational viscosity never reached a steady state, even up to Hencky strains of 5, unlike the behavior often seen for other polymer melts.[26,43] The LCP was stable up to $\epsilon = 5$, or elongations exceeding 140 times, but only forces measurable within the instrument sensitivity are reported. The transient elongational viscosity curves are replotted as a function of Hencky strain ($\epsilon = \dot{\epsilon}t$) in Figure 5. At low strains the transient elongational viscosity is weakly increasing with applied strain and weakly decreasing with increasing elongation rate. Above Hencky strains of 1, there is significant strain hardening behavior, with the viscosity collapsing onto the same "master curve". Within the scatter of the data, $\eta_\epsilon \propto \epsilon^2$ as $\epsilon$ exceeds 1.0. This scaling exceeds that expected for a Hookean solid, for which the elongational *stress* would scale linearly with strain, independent of strain rate. Here, the elongational stress increases linearly with strain rate and quadratic with the total applied strain. Note that there is no vertical shifting of the transient viscosity data, showing that the

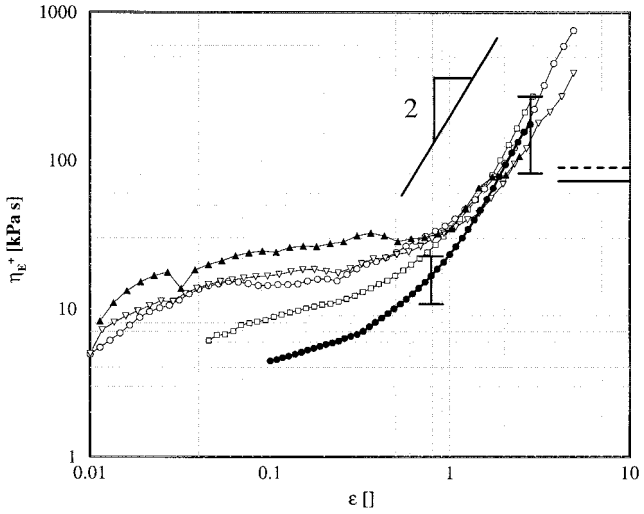


**Figure 5.** Elongational viscosity of Figure 4 replotted as a function of applied strain for elongational rates: $\dot{\epsilon} = 1.0\ s^{-1}$ (●); $\dot{\epsilon} = 0.3\ s^{-1}$ (□); $\dot{\epsilon} = 0.1\ s^{-1}$ (○); $\dot{\epsilon} = 0.03\ s^{-1}$ (▽); $\dot{\epsilon} = 0.01\ s^{-1}$ (▲). Also included as the horizontal lines at $\epsilon = 10$ are the fits from Doi theory, $S = 0.46$ (—) and $S = 0.736$ (- -). Characteristic error bars are shown.

material tends toward a fluid state that is truly independent of strain rate. This result suggests that the samples all reached the same state of molecular order, which must be highly oriented along the flow direction to be strain rate independent. Some evidence for strain scaling in lyotropic LCP solutions has been reported, but only by reducing the stress by the steady-state value.[28] Wilson and Baird noted that the shapes of their transient curves scaled with strain in the case of the HPC melt, but the magnitude of the viscosity deceased with increasing strain rate.[10] In the case of branched polyethylene (LDPE), the onset of strain hardening occurred above a critical strain, but the magnitude of the viscosity was still found to be a function of the applied strain rate.[24] A similar effect was also noted for branched polypropylene, where the strain hardening increased with decreasing strain rate.[27]

It should be noted that the shear viscosity was measured after a suitable preshear protocol, as was necessary to remove any loading structure. The samples for elongational measurements were not subjected to any such protocol, so the transient experiment starts with the material as loaded. Although these samples are not subjected to any undue loading stresses, we suspect that some of the variability of the elongational viscosity transients at short times may be a consequence of the sample preparation.

The transient viscosities are qualitatively, as well as quantitatively, different for the shear and elongational experiments. The shear transients exhibits an extreme over shoot before reaching a steady state, while the elongational transients do not exhibit an overshoot, and no steady state was observed up to the strains tested here.

The transient Trouton ratio

$$\eta_T^+ = \left.\frac{\eta_E^+(\epsilon,\dot{\epsilon})}{\eta^+(\gamma,\dot{\gamma})}\right|_{(\dot{\gamma}=\sqrt{3}\dot{\epsilon},\epsilon=\ln(\gamma+1))} \tag{6}$$

illustrates the non-Newtonian character and rheological uniqueness of this fluid. For simple polymers, such as LDPE, the transient Trouton ratio is close to the

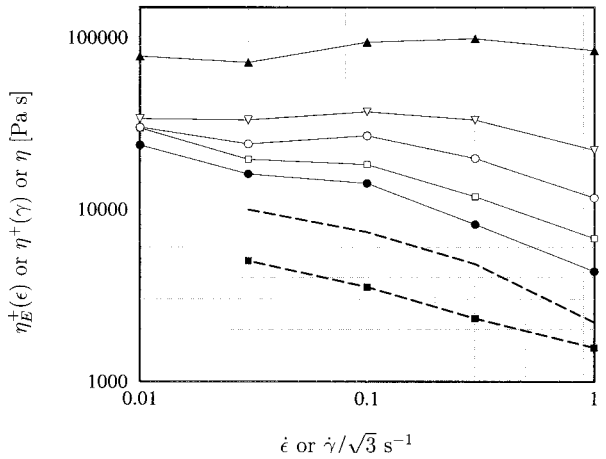


**Figure 6.** Transient elongational viscosity vs strain rate taken as a function of applied strain: $\epsilon = 0.1$ (●); $\epsilon = 0.3$ (□); $\epsilon = 0.6$ (○); $\epsilon = 1.0$ (▽); $\epsilon = 2.0$ (▲). Also included in the transient shear viscosity at $\gamma = 10$ (■), and the steady shear viscosity (- -).

expected Newtonian value of 3 for strains less than some critical strain. However, above the critical strain for hardening, the Trouton ratio can increase to the order of hundreds.[26] Metzner and Prilutski report Trouton ratios for a lyotropic LCP that exceed 3 but report no effect of strain.[9] For TLCPs, Wilson and Baird[10] (HPC,-Vectra A900) and Wagner et al.[29] (Vectra B950) report large Trouton ratios due to strain-hardening. Figure 6 shows a cross plot of the instantaneous viscosities at various elongations (strains) as a function of applied elongation rate (strain rate) for the TLCP. At low total Hencky strains, the transient elongational viscosities are parallel and higher than the corresponding steady shear viscosities, as well as the transient shear viscosities evaluated at $\eta^+(\gamma = 10)$, which are at strains lower than the shear stress overshoot. Increasing the elongational strain results in a marked increase in elongational viscosity and a loss of elongation-rate thinning. Both behaviors can be understood in terms of the degree of orientational order in the samples, as will be shown presently.

The extreme strain hardening observed here is of importance when processing TLCPs. It is reported that LCPs exhibit much lower flash than standard polymers,[2] making them useful for precision mold filling applications. The transient elongational viscosity data presented here support the possibility suggested by Wissbrun[2] that the large increase in elongation viscosity after small strains is the source of the low flashing. Previous work on lyotropic LCP solutions reported steady elongational viscosities,[9,28] unlike the strain-hardening transients seen in the current work, and that of Wilson and Baird[10] and Wagner et al.[29] This suggests that there is some fundamental difference between thermotropes and lyotropes. This difference leads to the same conclusion as reached by Metzner and Prilutski,[9] who noted that LCPs should be poor candidates for fiber spinning; however, for the TLCPs it is because of the prohibitively extreme strain-hardening, rather than the lack thereof observed in the lyotropes.

**Order Parameters.** X-ray scattering was performed on quenched samples from experiments covering a range of elongational rates and total elongational strain, as summarized in Table 1. The two-dimensional X-ray scattering intensity patterns are represented as iso-intensity contours in Figure 7, where the elongational

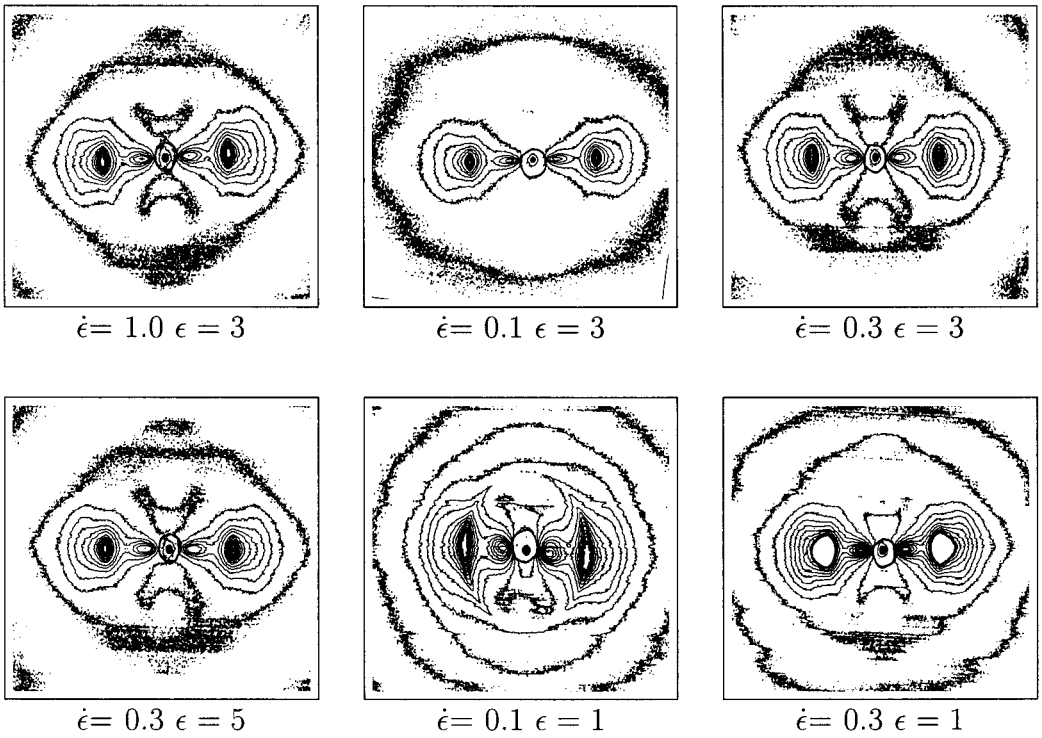


**Figure 7.** Isointensity contour plots from the 2D X-ray scattering for samples quenched at noted elongational rate and total strain. The elongation direction is vertical.

**Table 1. Measured Order Parameter Values for Indicated Elongational Rate and Strain[a]**

| | strain $\dot{\epsilon}t$ | | |
|---|---|---|---|
| rate $\dot{\epsilon}$ | 1 | 3 | 5 |
| 0.1 | 0.803 (10 s) | 0.962 (30 s) | |
| 0.3 | 0.854 (3.33 s) | 0.885 (10 s) | 0.910 (15 s) |
| 1.0 | | 0.925 (3 s) | |

[a] In parentheses is the time it takes to reach the desired strain.

direction is vertical on the page. There is anisotropy apparent in all of the samples.

The scattering angle for subsequent analysis was determined by generating a sector average I vs |**q**| plot for both 0° (horizontal) and 90° (vertical, and along fiber axis) azimuthal angle. A sample plot is shown in Figure 8, where the sector-averaged intensity was not corrected for constant background.

The scattering angle for maximum amplitude corresponds to $q = 1.42$ Å$^{-1}$ ($2\theta = 20.0°$) or a $d$ spacing of 4.4 Å. This peak is due to diffraction from lateral packing between polymer segments, as shown by Ishaq et al.[44] on a drawn, chemically similar copolyester (Vectra). Azimuthal scans were performed at this peak q position for each of the quenches. Normalized azimuthal intensities are shown in Figure 9 for the various quenches, where the intensity at zero angle was subtracted for purposes of comparison. Increasing sharpness of the peak with elongation rate and total strain corresponds to increasing orientational order of the LCP. The azimuthal scans are fit to eq 4 to extract $\alpha$, and the effective uniaxial order parameter $S_{\text{eff}}$ was calculated from eq 5. The $q$-independent background was extracted from a porod fit to the high angle scattering. Figure 10 shows a sample azimuthal scan and the corresponding

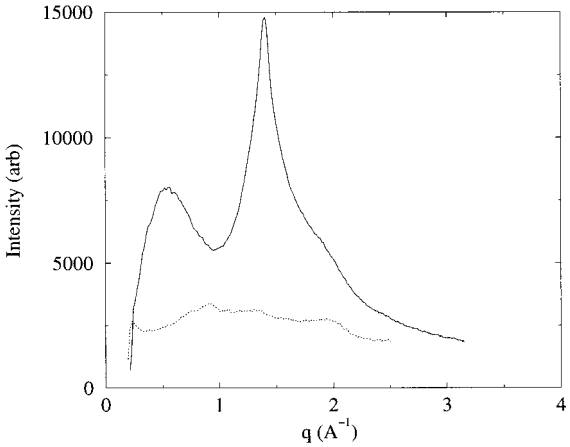


**Figure 8.** Sector averaged intensities vs q for quench sample with $\dot{\epsilon} = 0.3$ and $\epsilon = 3$. Higher intensity corresponds to the horizontal direction (perpendicular to the elongation).

parametric fit. Note that the fit is optimized for the higher intensities (fit range $135° \leq \Psi \leq 225°$) as the low intensity data is subject to greater uncertainty due to corrections for significant incoherent background and instrument scattering. Table 1 shows the calculated effective order parameter values obtained from the elongational quenches, with an uncertainty of $\pm 0.02$ for these highly ordered samples. The effective order parameters are an increasing function of strain, with little effect of strain rate. The values reach saturation around $\epsilon = 3$. Thus, the observation of a master curve for the elongational viscosity at large strains independent of strain rate is consistent with the measured saturation in the samples' molecular order at all strain rates.

These order parameters can be compared to the order expected from an affine deformation model, similar to

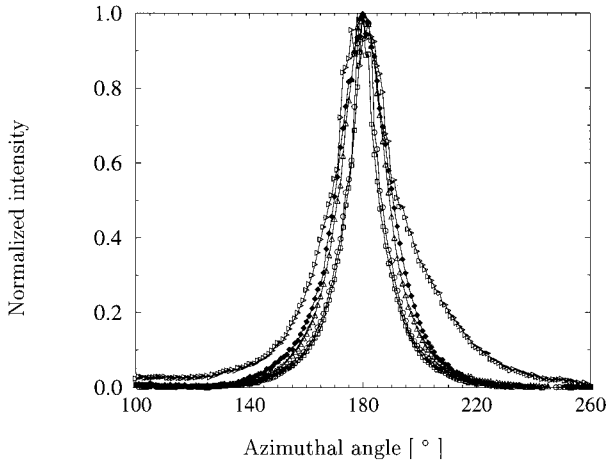


**Figure 9.** Normalized azimuthal intensity at peak $q$ position: $\dot{\epsilon} = 1.0$, $\epsilon = 3$ (○); $\dot{\epsilon} = 0.1$, $\epsilon = 3$ (□); $\dot{\epsilon} = 0.3$, $\epsilon = 3$ (◆); $\dot{\epsilon} = 0.3$, $\epsilon = 5$ (△); $\dot{\epsilon} = 0.1$, $\epsilon = 1$ (sideways open triangle).

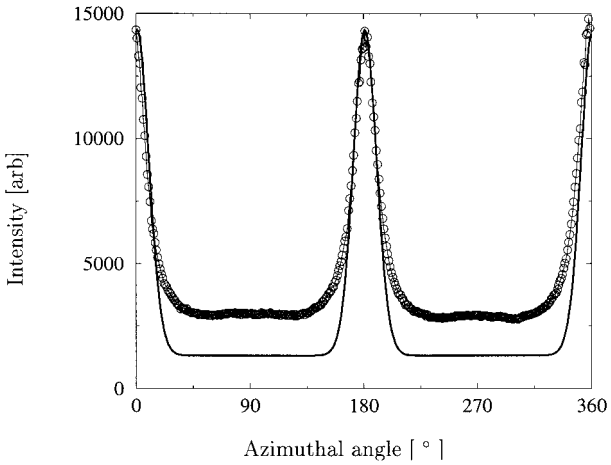


**Figure 10.** Azimuthal scan for sample with $\dot{\epsilon} = 0.3$ and $\epsilon = 3$, with corresponding parametric fit.

the approach of Picken et al.[45] Starting with an isotropic distribution of directors ($S = 0$) and then subjecting the director to an uniaxial deformation, an analytical expression

$$S = \frac{2a^3 + 1}{2(a^3 - 1)} - \frac{3a^3}{2(a^3 - 1)^{3/2}} \operatorname{atan}(\sqrt{a^3 - 1}) \quad (7)$$

where $a = \exp(\epsilon)$, describes the evolution of the macroscopic director as a function of strain.[45,46] Figure 11 shows the calculated macroscopic order parameter as a function of Hencky strain for uniaxial elongation. At low strain, the measured total order parameter is *higher* than that predicted from the affine deformation case. This enhancement in the order parameter could come from two sources not considered in the affine deformation physics, either the average initial state of the director is not isotropic, or there is some collaborative alignment between directors. The affine deformation predicts a macroscopic order parameter of 0.9 is reached by ≈2 Hencky strains, in agreement with the observed saturation of the order parameter.

A direct comparison can be made with the experimental results of van Eijnhoven-Rivera et al.[14] for the same TLCP in fully developed, isothermal capillary flow at a test temperature of 250 °C to ascertain how the order parameter depends on flow type. Table 2 summarizes their results for various capillary wall shear rates. The order parameters obtained in elongational flow exceed the shear results in all cases, demonstrating that elongational flow is superior for orienting main-chain LCPs, even though the shear rates tested were orders of magnitude higher than the elongational rates. Also, the very high order parameters obtained under elongational flow reflect a significant coupling of the flow to the *molecular order* in the polymer. Shear flow is predicted to affect the *molecular* order parameter only in region III, whereas low flow rates affect the net, overall order parameter either by inducing tumbling or aligning the mesoscale texture, as has been demonstrated.[12,17] Assuming the order parameter obtained under high shear flow (≈0.46) to be indicative of the *molecular* order parameter in the nematic demonstrates that elongational Hencky strains of order 1 are sufficient to orient the TLCP molecules themselves. If, however, one takes the extensional data to reflect the molecular order parameter (≈0.9), then shear flows of much higher rates are shown to be unable to overcome the disorganizing influence of texture or tumbling.

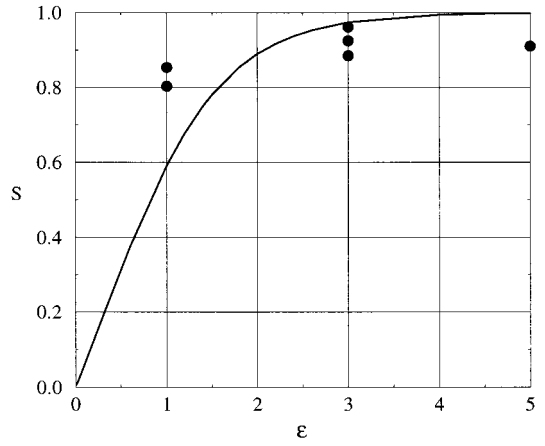


**Figure 11.** $S$ for affine elongational deformation in terms of $\epsilon$ as derived by Picken et al.[45] Also included is $S$ as measured for the elongated LCP for various values of $\epsilon$ (●).

**Table 2. Order Parameters Obtained in Steady Shear Flow by van Eijnhoven-Rivera et al.[14] on the Same TLCP**

| $\dot{\gamma}$ ($s^{-1}$) | $S$ |
|---|---|
| 60 | 0.39 |
| 620 | 0.47 |
| 1360 | 0.46 |
| 3100 | 0.45 |

## Comparison to the Doi Model

Transient elongational viscosity predictions of the molecular model of rigid rods in solution as proposed by Doi[6] do not exhibit the strain-hardening behavior seen in our TLCP system.[10,28] However, given the extensive rheological characterization and independent measurement of the order parameters, it is useful to test the model's ability to predict any of the measured elongational behavior of TLCPs. The Doi theory[6] describes the dynamics of rodlike polymers in concentrated solutions. The model has three parameters, c, the concentration, $\bar{D}_r$, a modified rotational diffusion coefficient, and S, the order parameter. These parameters all have physical meaning in lyotropic LCPs, and for thermotropes the physics remains the same with temperature playing the role of concentration.

**Table 3. Molecular Model Predictions of the Trouton Ratio and Elongational Viscosity, $\eta_E$**

| $S$ | Trouton ratio | $\eta$ (kPa·s) | $\eta_E$ (kPa·s) |
|---|---|---|---|
| 0.46 | 5 | 14.8 | 73 |
| 0.74 | 10 | 9 | 90 |

For the limit of low shear,[6,9] the first normal stress difference ($N_1$) is given by

$$N_1 = \frac{ck_bT}{2\bar{D}_r}\left(\frac{(1-S)^{3/2}(1+2S)^{1/2}(1+3S/2)S}{(1+S/2)^2}\right)\dot{\gamma} \quad (8)$$

the shear viscosity ($\eta$) is

$$\eta = \frac{ck_bT}{6\bar{D}_r}\left(\frac{(1-S)^2(1+2S)(1+3S/2)}{(1+S/2)^2}\right) \quad (9)$$

and the Trouton ratio is

$$\frac{\eta_E}{\eta} = \frac{3(1+S/2)^2}{(1-S)(1+3/2S)} \quad (10)$$

In the low shear limit, the steady viscosity and $N_1$ values from Figure 1 follow the scaling predicted by the model, specifically that $N \propto \dot{\gamma}$. In this region, the ratio of viscosity to $N_1$ allows S = 0.736 to be fitted using eqs 8 and 9. Alternatively, the value of $S = 0.46$ (the value obtained via WAXS under high shear from van Eijnhoven-Rivera et al.[14] coupled with the $N_1$ data can be used to calculate $\eta = 14.8$ k, which although higher than the measured $\eta \approx 9$k is not unreasonable. The $N_1$ curve deviates from the linear scaling with shear rate beyond $\approx$0.2, indicating that $\bar{D}_r \leq 0.2\ s^{-1}$.

The two methods of fitting the shear rheology to the model lead to two predictions for the Trouton ratio, calculated from eq 10, as summarized in Table 3. Also in Table 3 is the elongational viscosity resulting from the Trouton ratio times the shear viscosity. The calculated elongational viscosities are marked in Figure 5, indicating the predicted steady-state values if the sample were an idealized, rigid-rod nematic. As seen, the measured viscosities appear to asymptote toward the predicted, steady-state viscosities but are preempted from achieving them by the onset of extreme strain hardening. This qualitative observation appears valid until some missing physics associated with an additional microstructure drives strain hardening is taken into account.

The physical basis for such strain-hardening in TLCPs is not explicitly considered in the physics of the Doi model and does not naturally arise for a fluid of rigid rods. Therefore, other effects, such as defects, chemical inhomogeneities, flexibility or branching, or strain-induced crystallization, dominate the rheology at higher elongational strains. Visual observations of samples taken before elongation and quenched at high elongations were made using cross-polarized optics in a Nikon photostat microscope at 250 °C. Samples taken at rest exhibit a random defect texture evident as snakelike defect lines. At high elongational strains, the samples (which have been quenched and remelted) are also fluidlike, but exhibit bands oriented orthogonal to the draw direction, similar to images published by Riti and Navard.[47] No evidence of crystallization or other visible changes in the samples' homogeneity were evident, suggesting the strain hardening may be associated with organization of the defect texture. The defect texture is known to play an important role in the low shear rheology of LCPs;[11,17] thus, it is a challenge for future investigations to determine if it could also be responsible for the strain-hardening observed here and by others.

## Conclusion

As noted over a decade ago by Metzner and Prilutski, liquid crystalline polymers represent a "rheologically distinct class of materials" [9] that exhibit a very complex transient rheological response. As demonstrated here for elongational flows, as well as for shear flows as documented in many of the references herein, direct measurements of the molecular and mesoscale order can be used to rationalize, and sometimes even quantitatively predict, this complex rheological behavior. We find, however, some important differences between measurements on an industrial thermotropic LCP and reports for lyotropic LCPs and models of idealized, rigid rod nematic fluids. Most notably, the TCLP investigated here exhibits extreme elongational strain-hardening that results in very high Trouton ratios for Hencky strains greater than one. Measurements of the net molecular order parameter support the observed scaling in that the samples' molecular order saturates in the strain-hardening regime, independent of the applied strain rate. The suggestion is made that the defect texture may be responsible for the observed rheological discrepancies, although flexibility and other issues associated with the complex chemical composition cannot be ruled out. The successful understanding of these two distinct flow types is relevant to designing processing strategies for obtaining optimal processing and final material properties for LCP based materials.

**Acknowledgment.** We thank and acknowledge Dr. G. Alms and Dr. R. Soelch of DuPont Engineering Polymers for material support and guidance. The authors thank Prof. Dr. H. C. Öttinger, Prof. Dr. J. Meissner, D. Rohr, and Dr. T. Schweizer all of the Institute for Polymers of the Swiss Federal Institute of Technology (ETH), Zürich, Switzerland where the RME measurements were performed. We acknowledge Dr. M. van Eijndhoven-Rivera of Dupont CR&D for performing the X-ray scattering and Dr. Ben Hsiao (SUNY Stonybook) for useful discussions. Financial support for this project was provided by DuPont Engineering Polymers, the Delaware Research Partnership, the National Science Foundation (Grant No. CTS-9158146, and INT-9400209), and the ETH Zürich.

## References and Notes

(1) Committee on Liquid Crystal Polymers. *Liquid Crystalline Polymers*; Technical Report NMAB−453; National Material Advisory Board, National Research Council: Washington, DC, 1990.
(2) Wissbrun, K. F. *Polym. Eng. Sci.* **1991**, *31*, 1130.
(3) Dutta, D.; Fruitwalai, H.; Kohlii, A.; Weiss, R. A. *Polym. Eng. Sci.* **1990**, *30*, 1005.
(4) Mewis, J.; Moldenaers, P. *Curr. Opin. Colloid Interface Sci.* **1996**, *1*, 466.
(5) Marrucci, G.; Greco, F. In *Advances in Chemical Physics*; Wiley: New York, 1993; Vol. 86.
(6) Doi, M. *J. Polym. Sci.: Polym. Phys. Ed.* **1981**, *19*, 229.
(7) Larson, R. G.; Doi, M. *J. Rheol.* **1991**, *35*, 539.
(8) Maffettone, P. L.; Marrucci, G.; Mortier, M.; Moldenaers, P.; Mewis, J. *J. Chem. Phys.* **1994**, *100*, 7736.
(9) Metzner, A. B.; Prilutski, J. *J. Rheol.* **1986**, *30*, 661.
(10) Wilson, T. S.; Baird, D. G. *Journal of Non-Newtonian Fluid Mech.* **1992**, *44*, 85.
(11) Walker, L. M.; Wagner, N.J. *J. Rheol.* **1994**, *38*, 1525.

(12) Hongladarom, K.; Ugaz, V.; Cinader, D.; Burghardt, W. R.; Quintana, J. P.; Hsiao, B. S.; Dadmum, M. D.; Magid, L. J. *Macromolecules* **1996**, *29*, 5346.
(13) Picken, S. J.; Aerts, J.; Visser, R.; Northolt, M. G. *Macromolecules* **1990**, *23*, 3849.
(14) van Eijndhoven-Rivera, M. J.; Wagner, N. J.; Hsiao, B. *J. Polym. Sci.: Part B Polym. Phys.* **1998**, *36*, 1769.
(15) Radler, M. J.; Landes, B. G.; Broomall, C. F.; Chritz, T. C.; Rudolf, P. R.; Mills, M. E.; Bubeck, R. A. *J. Polym. Sci.: Part B Polym. Phys.* **1994**, *32*, 2567.
(16) Moon, H.; Park J.; Liu J. *J. Appl. Polym. Sci.* **1996**, *59*, 489.
(17) Walker, L. M.; Kernick, W. A.; Wagner, N. J. *Macromolecules* **1997**, *30*, 508.
(18) Bedford, B. D.; Burghardt, W. R.; *J. Rheol.* **1996**, *40*, 235.
(19) Petrie, C. J. S *Elongational flows: Aspects of the behaviour of model elasticoviscous fluids*; Pitman: London, 1979.
(20) Gupta, R. K.; Sridhar, T. In *Rheological Measurement*; Collyer, A. A., Clegg, D. W., Eds.; Elsevier Applied Science: New York, 1988.
(21) Meissner, J.; Hostettler, J. *Rheol. Acta* **1994**, *33*, 1.
(22) Gramespacher, H.; Meissner, J. *J. Rheol.* **1997**, *41*, 27.
(23) Levitt, L.; Macosko, C. W.; Schweizer, T.; Meissner, J. *J. Rheol.* **1997**, *41*, 671.
(24) Münstedt, M.; Laun, H. M. *Rheol. Acta* **1981**, *20*, 211.
(25) Münstedt, H.; Laun, H. M. *Rheol. Acta* **1979**, *18*, 492.
(26) Laun, H. M.; Schuch, H. *J. Rheol.* **1989**, *33*, 119.
(27) Hingmann, R.; Marczinke, B. L. *J. Rheol.* **1994**, *38*, 573.
(28) Ooi, Y. W.; Sridhar, T. *Ind. Eng. Chem. Res.* **1994**, *33*, 2368.
(29) Wagner, M. H.; Ixner, Th.; Geiger, K. *J. Rheol.* **1997**, *41*, 1087.
(30) Waggoner M. G.; Samuels M. R. Thermotropic liquid crystalline polyester compositions. United States Patent 5 110 896, 1992.
(31) Soelch, R. DuPont, private communication.
(32) Agrawal, P. K.; Lee, W. K.; Lorntson, J. M.; Richardson, C. I.; Wissbrun, K. F.; Metzner, A. B. *Trans. Soc. Rheol.* **1977**, *21*, 355.
(33) Jones, D. M.; Walter, K.; William, P. R. *Rheol. Acta* **1987**, *26*, 20.
(34) Wissbrun, K. F.; Kiss, G.; Cogswell, F. N. *Chem. Eng. Commun.* **1987**, *53*.
(35) Rivera-Gastélum M. J.; Wagner N. J. *J. Polym. Sci.: Part B Polym. Phys.* **1996**, *34*, 2433.
(36) Kalika, D. S.; Giles, D. W.; Denn, M. M. *J. Rheol.* **1990**, *34*, 139.
(37) Asada, T.; Onogi, S.; and Yanase, Y. *Polym. Eng. Sci.* **1984**, *24*, 355.
(38) Baek, S. G.; Magda, J. J.; Larson, R. G. *J. Rheol.* **1993**, *37*, 1201.
(39) Kiss, G.; Porter, R. S. *J. Polym. Sci.: Polym. Phys. Ed.* **1978**, *65*, 198.
(40) Moldenaers, P.; Mortier, M.; Mewis, J. *Chem. Eng. Sci.* **1994**, *49*, 699.
(41) Mewis, J. and Moldenaers, P. *Mol. Cryst. Liq. Cryst.* **1987**, *153*, 291.
(42) Beekmans, F.; Gotsis, A. D.; Norder, B. *J. Rheol.* **1996**, *40*, 947.
(43) Laun, H. M.; Munstedt, H. *Rheol. Acta* **1978**, *17*, 415.
(44) Ishaq, M.; Blackwell, J.; Chvalun, S. N. *Polymer* **1996**, *37*, 1765.
(45) Picken, S. J.; van der Zwaag, S.; Northolt, M. G. *Polymer* **1992**, *33*, 2998.
(46) Kuhn, v. W.; Grün, F. *Kolloid Z.* **1942**, *101*, 248.
(47) Riti, J. B.; Cidade, M. T.; Godinho, M. H.; Martins, A. F.; Navard, P. *J. Rheol.* **1997**, *41*, 1247.

MA980780K